

TESTING AND ANALYSIS OF A HIGHLY LOADED COMPOSITE FLANGE

Jansson N.E.¹, Lutz A.², Wolfahrt M.³, and Sjunnesson A.¹

¹ Volvo Aero Corporation, SE 461 81 Trollhättan, Sweden

² Fischer Advanced Composite Components AG, A-4910 Ried im Innkreis, Austria

³ Polymer Competence Center Leoben GmbH, A-8700 Leoben, Austria

niklas.nj.jansson@volvo.com

ABSTRACT

In a part of the EnVIronmenTALly Friendly Aero Engine (VITAL) project within the EU FP6 program, Volvo Aero Corporation and Fischer Advanced Composite Components and other partners are developing a composite bypass structure for a jet engine. The structure contains a highly loaded vertical flange connecting the bypass structure to the fan case. In this paper is the manufacturing of a section of that flange using Non Crimp Fabrics and a liquid injection moulding technique described. The flange section is subsequently cut into specimens and the strength and failure modes are experimentally determined. The experimental results are compared to finite element simulations for both stiffness and failure load levels and a good correspondence is shown.

1. INTRODUCTION

Modern civil jet engines are growing in size compared to the thrust they produce to improve fuel consumption and reduce noise. To compensate the potential weight increase, fan outlet guide vanes (OGVs) with aerodynamic function are combined with the load carrying function of struts previously used in engine designs. In addition, a material change from aluminium or titanium to composite material is investigated. The OGVs are located in the engine by-pass duct between the outer case and the core engine at the inner diameter, see Figure 1a.

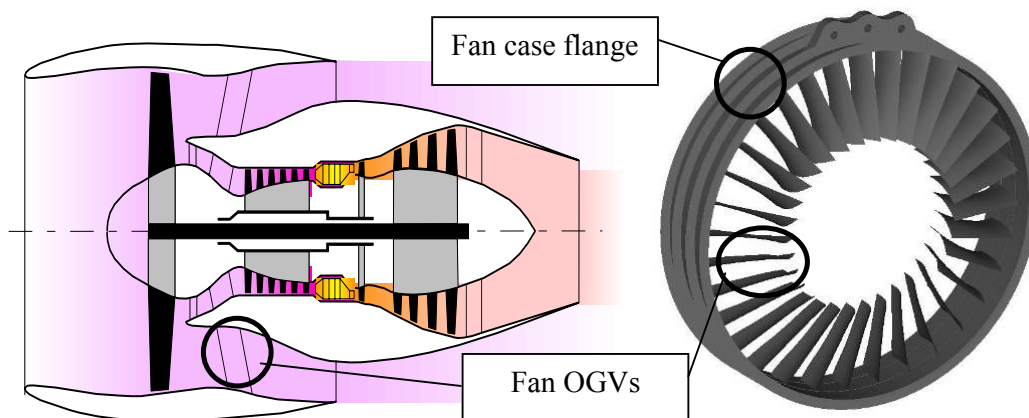


Figure 1: (a) Typical jet engine with fan OGVs, ref 1. (b) Composite bypass structure

In metallic structures, the bypass structure is connected to the fan case by a vertical flange and bolted joints. Although this is not an optimal configuration for a composite flange it was still chosen also for the composite case in order to be compatible with existing configurations (see circle in Figure 1b.). During extreme loading conditions, i.e. a Fan Blade Out (FBO) event where a fan blade is lost, strikes the fan case and

causes large unbalance forces in the engine, the fan case to bypass structure flange will be highly loaded. If one recalculates the forces and moments on the flange to tensile forces per meter, the loading is estimated to be in the order of 120 kN/m.

The objectives of the work are to demonstrate the strength potential of a composite flange as well as to verify the prediction accuracy of the finite element simulations.

In the first section of the paper, the geometry, material and the manufacturing route of the flange specimen is described. In the following sections, descriptions of the test-setup and the analysis approach are given. The paper is concluded with a result section comparing the test and analysis results and a conclusion section.

2. FLANGE SPECIMEN MATERIALS AND MANUFACTURING

The specimens were manufactured by cutting out small flange specimens from a sector of the ring flange. A special metal mould with a flange on each side was used. The length of the mould was about 800 mm.

A number of dry preforms were prepared (basically of rectangular shape) to be draped into the mould. The preforms used for the manufacturing were combinations of Biax and Triax NCF's (non-crimp fabrics) made out of carbon fibres giving fibre angles of $\pm 45/90$ with the 0-direction in the circumferential direction. A special characteristic of the specimens is the backing plate located on the inner side of the flanges. Its task is to reinforce the radius and to improve the strength of the part. After the lay up of the flange section was finished, the material for the backing plate was draped into the flange directly onto the other material. So the backing plate is completely integrated and cocured with the flange.

For the infusion of the part a RIFT process (Resin infusion under flexible tooling) was used. After the bagging procedure was completed, the tool was put in upright position and inserted into an oven (cp. Figure 2a). The infusion was carried out with a one part epoxy resin and a corresponding standard cure cycle. After curing the flange had a thickness of 12.5 mm (including backing plate of 4mm, see Figure 2b) and 50% FVF (fibre volume fraction).

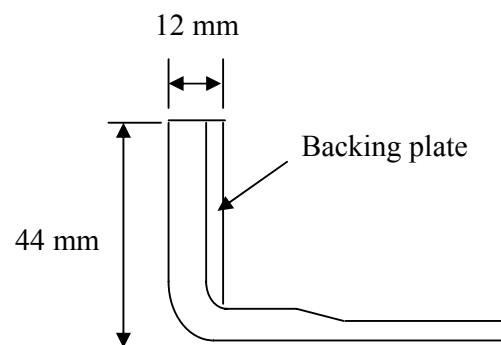


Figure 2 (a) Bagged flange on tool before resin injection (b) Sketch of flange cross-section

After demoulding the part (cp. Figure 3) the specimens were cut out at predefined positions with a width of 33 mm and prepared for the tests.



Figure 3 Flange section after demoulding

3. TEST PROCEDURE

Tensile tests were conducted using a Zwick Z250 universal tensile-compression testing machine (Zwick GmbH & Co. KG, Ulm, D) with wedge-screw grips to determine the tensile force values until the first decay in the load-crosshead displacement curves of the specimens. All tests were performed at a cross-head speed of 2 mm/min according to ASTM D3039 [2] in a laboratory environment of 23°C and 50% relative humidity. In addition, to determine the local strain distribution of the test specimens in relation to the support structure, optical full-field strain measurements were performed using the 3D image correlation photogrammetry system ARAMIS (GOM, Braunschweig, Germany). For this purpose a stochastic dot pattern was applied on the side of all specimens by using an aerosol spray. Prior to testing the system was calibrated with special calibration plates to correct distortions of the lenses and to calibrate the position of the cameras to each other.

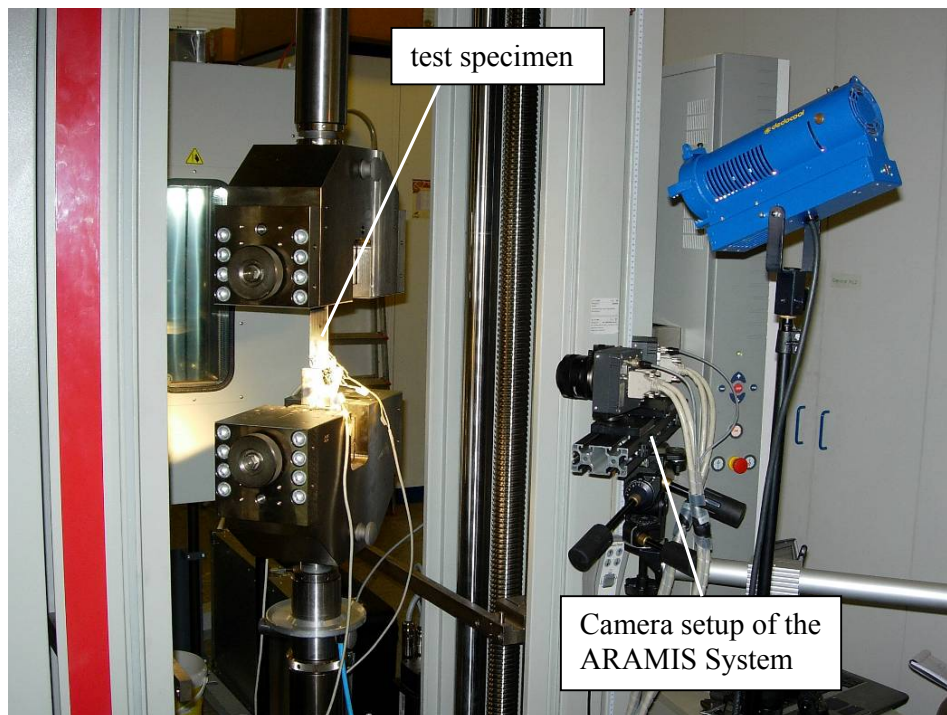


Figure 4: Test setup for the tensile tests.

The test setup used for the investigations is depicted in Fig. 4. In order to fix the specimens to the support structure hexagon head screws (DIN EN ISO 4017 M8x50-10.9) were selected.

4. ANALYSIS

The finite element analysis has been performed with Ansys 11.0 using layered solid elements type 186 for the composite parts. The mesh used is shown in Figure 5. As can be seen six elements are used through the thickness throughout the specimen. Each colour denotes a component where the section properties are given by that the actual stack of material plies are split in six equally thick stacks. In the model, actual material plies are hence divided between the component section stacks when the numbers of plies are not a multiple of six.

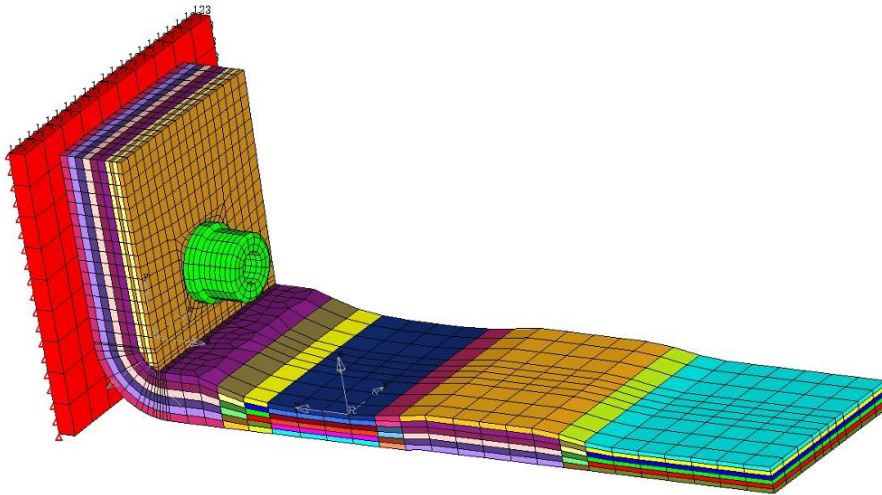


Figure 5 FE-model of the flange test specimen

The support structure is represented by a steel plate constrained at the backside in all degrees of freedom and with contact elements at the interface to the composite flange. The bolt is modelled including pretension and contact elements between the bolt head and the composite flange. Loading is accomplished by applying a force to a rigid element at the end of the specimen, at this location the rotation is also constrained representing a clamped boundary condition.

The composite ply properties used are estimated from literature data (mainly from ref [3]) and are given in Table 1 whereas a modulus of 210 GPa is used for the bolt and support structure

Stiffness properties [GPa]	E_1	$E_2=E_3$	$G_{12}=G_{13}$	G_{23}	$\nu_{12}=\nu_{13}$	ν_{23}
	130	9.5	3.3	3.1	0.25	0.4
Strength Properties [MPa]	σ_{11t}	σ_{11c}	$\sigma_{22t}=\sigma_{33t}$	$\sigma_{22c}=\sigma_{33c}$	$\tau_{12}=\tau_{13}=\tau_{23}$	
	2000	1000	50	250	70	

Table 1 Estimated ply properties where subscript 1 refers to fibre direction, 2 to the in-plane transverse direction and 3 to the through thickness direction

For the prediction of failure, the Tsai-Wu criterion implemented in Ansys is used with the biaxial stress coupling terms set to zero, see ref [4] for details. There are two options for the post processing of the Tsai-Wu criterion in Ansys, the strength index

and the inverse of the strength ratio index, in this work the latter has been used. If the stresses are described by the base stress state and a load factor α , the failure is assumed to occur when $\alpha=1$, for a general stress state σ_0 the following applies

$$\sigma = \alpha \sigma_0; \text{ Strength ratio} = 1/\alpha \begin{cases} < 1 \text{ No failure} \\ \geq 1 \text{ Failure} \end{cases}$$

Note that this criterion is linear so that the strength ratio α directly gives how much the loads can be increased before failure.

5. RESULTS

5.1 Finite element results

In Figure 6 the inverse of the strength ratio index is shown for the first predicted failure. This failure is due to a through thickness dominated stress state in the interface between the flange and the integrated backing plate at the tip of the backing plate. As the mesh (especially in the backing plate) is coarse and hence the stresses not resolved, the predicted failure is said to occur somewhere inbetween that the first point validates the failure criterion and when the area of failure extends over approximately an element width. With this approach, failure is predicted in a load band between 8 and 9 kN.

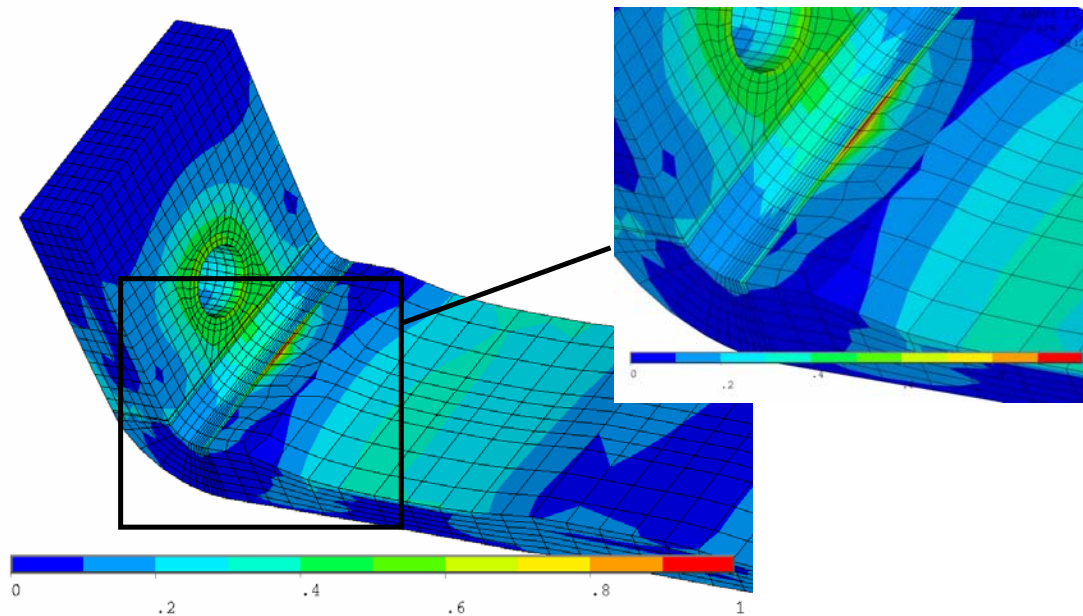


Figure 6 Predicted failure (strength ratio >1) at the backing plate to flange interface at ~8-9 kN

The corresponding predicted deformation is shown in Figure 7. Note that the selected distance to the gripping allows a large rotation of the bend which in turns gives a comparably low tensile stress in the above mentioned interface, it is expected that a more general load case with radial forces and a constraint closer to the flange would lead to an earlier interface failure

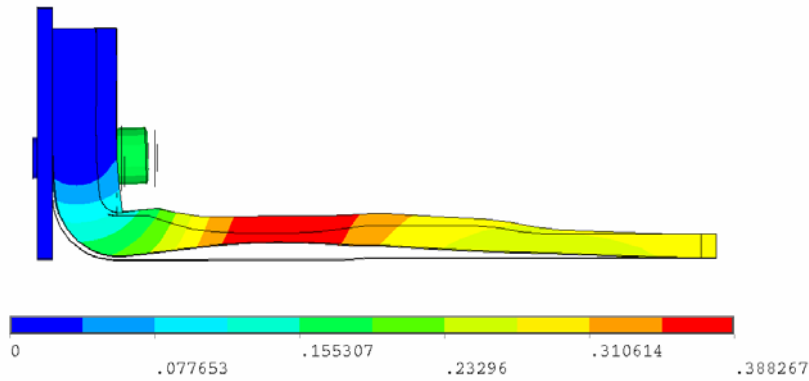


Figure 7 Deformation in mm of the structure at a load of 10 kN (scale factor 10)

This first predicted failure mode does not constitute fatal (final) failure. Since a considerable shear stress exists in the backing plate to flange interface, it is likely that a delamination will grow in the interface. As this is difficult to simulate explicitly it is here assumed that the backing plate totally and instantly debonds from the flange. To take this into account in the simulations a second run is performed with the backing plate detached from the flange and contact conditions specified on the interface.

The predicted failure in the simulation with debonded backing plate is a transverse shear dominated failure in the upper part of the radius beneath the hole, this is shown in Figure 8 where the element layer 4 (counted from the support structure side) is displayed. This happens at a load of ~ 19 kN. This is expected to lead to delaminations in the flange region at continued loading.

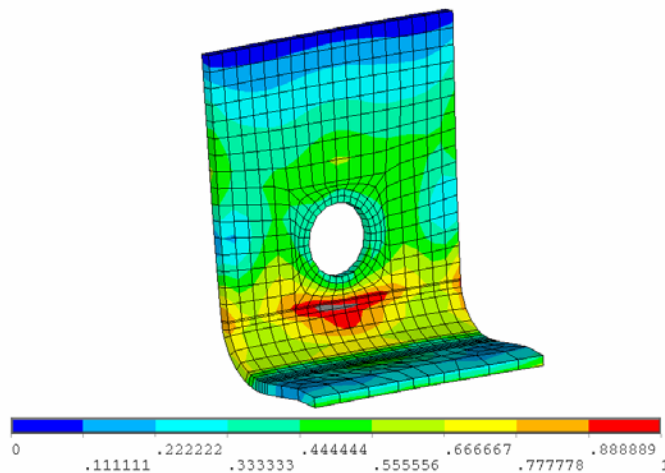


Figure 8 Transverse shear dominated failure (strength ratio < 1) in element layer four in the interior of the upper end of the bend radius

5.1 Comparison of experimental and FE-results

The load versus cross head displacement is shown in Figure 9 for the four specimens tested. All the curves look similar even though there is some scatter in the maximum force value which varies between ~ 18 - 22 kN. A slightly non-linear response starting at roughly 10 kN can also be discerned, this is shown more in detail in Figure 10 where the displacements with respect to the support structure of a point (denoted by A), located at the edge of the specimen just above the radius, are shown for two specimens.

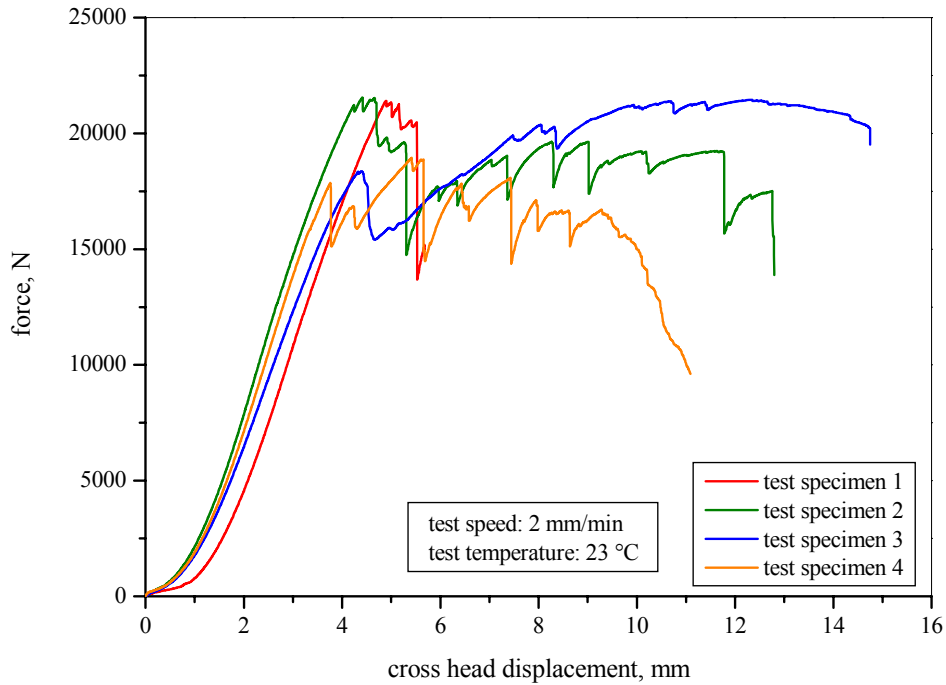


Figure 9: Experimental force versus cross head displacement curves for test specimen 1 to 4.

The figure also shows the simulated displacements with bonded and debonded backing plate plotted together with the estimated failure loads as a band for the debonding and a line for the failure. When the jump on the spec 2 curve is treated as an artifact from the testing and measurement and neglected, it seems like the experimental curves starts with stiffness similar to the bonded FE case, at a load of ~10 kN the stiffness changes and approaches the stiffness of the debonded specimen before softening close to ultimate load.

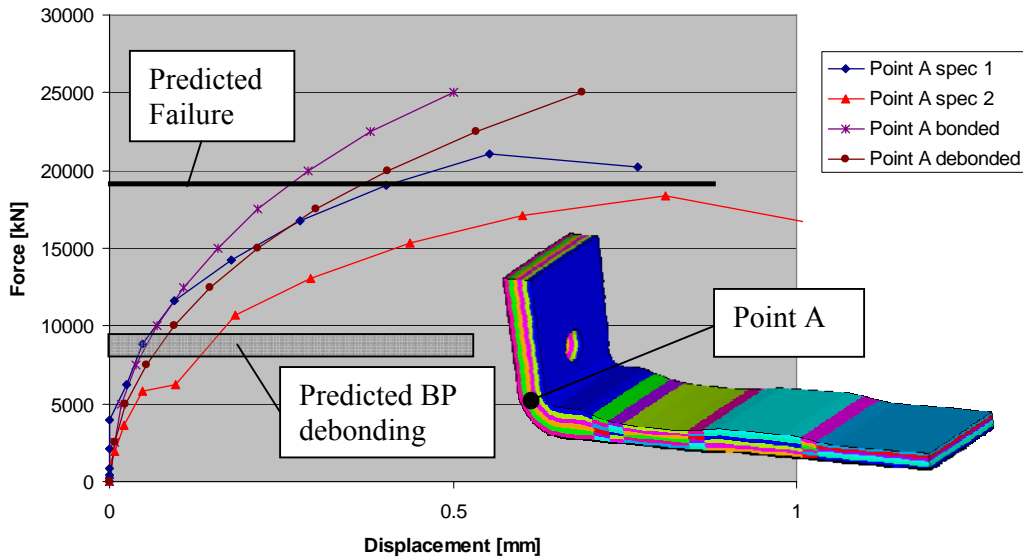


Figure 10 Comparison measured vs. predicted displacement of point A

To verify that the load drop after ultimate load is due to delaminations in the flange radius rather than e.g. bolt plasticity, one specimen were stopped just after the load drop and inspected. This showed that the backing plate was indeed debonded and that the flange radius was delaminated, see figure 11.

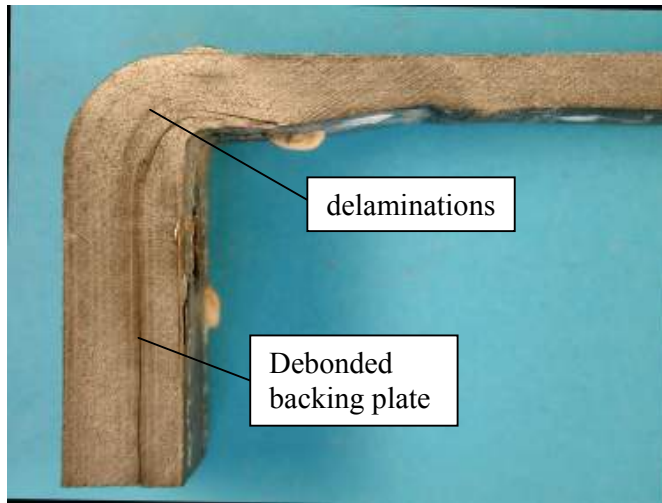


Figure 11 Picture of specimen 1 after test stopped just past maximum load

6. CONCLUSIONS

In the workpackage dealing with composite structures in the VITAL project, a composite bypass structure with integrated outlet guide vanes and an outer casing has been designed. For the attachment to the fan case, a vertical flange is incorporated in the outer casing. A section of this flange has been manufactured using NCF's and a liquid moulding technique. The section was cut into specimens, instrumented and structurally tested in a tensile test machine. The experimental results have been compared to results from finite element simulations using only basic material data and a good correlation was found. Also, the predicted failure modes from the simulations were verified from the tests. This work shows that it is feasible to design and manufacture a fan case flange strong enough to withstand expected ultimate loads.

ACKNOWLEDGEMENTS

The work presented in this paper has been funded in part by the CEC in the FP6 project VITAL (project no. AIP-CT-2004-012271) under contract number 012271. The authors would also like to thank Mr. Michael Jerabek from the Polymer Competence Center Leoben GmbH (Leoben, Austria) for his support with the ARAMIS-System and for participating in the experimental work.

REFERENCES

- 1- Kurzke J., User's Manual 9 Gasturb 9, 2001.
- 2- ASTM D3039 (2000): "Standard Test Method for Tensile Properties of Polymer Matrix Composites", American Society for Testing and Materials (West Conshohocken, USA)
- 3- Composite Materials Handbook, Volume 3. "Polymer Matrix Composites Materials Usage, Design and analysis", *MIL-HDBK-17-3F, Volume 3 of 5*, 17 June 2002
- 4- "Release 11.0 Documentation for ANSYS", ANSYS Inc, 2007